PROS AND CONS OF LOW-FIELD MAGNETIC RESONANCE IMAGING IN VETERINARY PRACTICE

MARTIN KONAR, JOHANN LANG

Low-field (LF) (0.2–0.4 T) magnetic resonance (MR) imaging predominates in veterinary practice. Advantages of LF MR include reduced costs, better patient access, and greater safety. High quality examinations can be achieved using appropriate protocols and investing more scanning time than with high-field (HF) systems. The main disadvantage of LF MR is the reduced signal to noise ratio compared with HF systems. LF MR protocols for small animal brain and spine imaging are described. © 2011 *Veterinary Radiology & Ultrasound, Vol. 52, No. 1, Supp. 1, 2011, pp S5–S14.*

Key words: brain, dog, low-field, magnetic resonance imaging.

Introduction

THE DEFINITION OF high-field (HF), mid-field (MF), and low-field (LF) magnetic resonance (MR) imaging is vague and has tended to change over time.[1,2] For this review we use LF MR to mean field strengths of 0.2–0.4 T. It is difficult to describe in detail the distribution of magnetic field strengths in veterinary use; however, there are more MR scanners installed in private practices than in veterinary schools, and in private practices LF scanners predominate. LF MR imaging has been used extensively for veterinary patients with intracranial, spinal, and musculoskeletal conditions.[3–13]

Overview of Systems

In veterinary practices there are examples of dedicated veterinary LF MR scanners and LF MR scanners produced for human use (Table 1). Manufacturers designing systems for veterinary use usually offer adapted software (e.g., adapted slice orientation on the display, the possibility to insert species, and breed information), receiving coils optimized for veterinary anatomy, and specific applications support for veterinary needs. Purchase and maintenance costs are usually lower for veterinary than for human MR systems, but lower prices are accompanied by lower specifications, such as lower gradient slew rate and smaller volume of homogenous magnetic field, which limits the maximal field of view (FOV). Veterinary MR manufacturers are continually improving the specifications of their systems to compete with MR systems designed for humans, which tend to be more expensive, have better magnetic field homogeneity, larger FOV, stronger gradients (slew rate), multichannel receiver coils, and more recent sequences, such as diffusion-weighted imaging (DWI). However, potential disadvantages of MR systems designed for humans include coil design adapted to human anatomy (e.g., thorax, shoulder), software adapted for humans (e.g., patient data, slice orientation), and less enthusiasm for addressing special veterinary needs (e.g., adapting coil design).

Limitations of LF MR

The fundamental limitation of LF MR is the reduced signal to noise ratio (SNR) compared with HF MR imaging. This is generally associated with longer scan times and decreased resolution leading to less pretty, but usually still diagnostic images.[14–17] Exceptions include special indications such as multiple sclerosis[18,19] and high-resolution musculoskeletal imaging.[20,21] Direct comparisons between images of equine cadaver limbs obtained using different magnetic field strengths found similar results.[22,23]

The compact magnet design of some veterinary scanners may not allow scanning of the caudal cervical or cranial thoracic spine in large dogs (from about 50 kg). Similarly in these scanners a small maximal FOV (around 15 cm) may necessitate frequent patient repositioning when examining the spine, thus making it more time consuming than with larger FOV systems. Total body LF MR imaging can be performed with high diagnostic accuracy,[24] but is either very time consuming or must be limited to overview sequences. Even at 1.5 T, a total body MR protocol for imaging canine cancer patients requires 60–75 min.[25]

Susceptibility effects are less at low magnetic field strengths, hence the appearance of hematomas is different[26–28] and the sensitivity of T2*-weighted images for detecting small foci of hemorrhage is decreased compared

From the MR Support Service, Ripa di Seravezza 55047, Italy (Konar) and the Department of Clinical Veterinary Medicine, Division of Clinical Radiology, Vetsuisse Faculty, University of Berne, Berne CH-3012, Switzerland (Lang).

Address correspondence and reprint requests to Martin Konar, at the above address. E-mail: martinkonar@hotmail.com

Received July 5, 2010; accepted for publication October 28, 2010.
doi: 10.1111/j.1740-8261.2010.01780.x

TABLE 1. Overview on Available Low Field MRI Scanners

	Dedicated Veterinary Systems				Open Human Medicine Systems						
Manufacturer	Esaote		Paramed	Hallmarq	Hitachi			Siemens		GE	
System	VetMR	VetMR Grande	MrV	EQ2 (Standing Equine MRI)	Airis Mate	Airis Vento	Aperto (Eterna)	Concerto	Magnetom C	Signa Profile	Signa Ovation
Field strength (T)	0.2	0.25	0.22	0.27	0.2	0.3	0.4	0.2	0.35	0.2	0.35
Gradient strength (mT/m)	20	20	15	20	15	21	22	20	24	19	19
Gradient slew rate (mT/m/s)	25	25	25	100	30	55	55	NA	55	46	55

Philips and Toshiba do not offer low-field MRI systems on their website.MRI, magnetic resonance imaging.

with HF MR.[29–32] Nevertheless, signal loss of hemorrhagic lesions on T2* weighting in comparison with T2 can be demonstrated in LF MR images (Fig. 1).

DWI can be performed with LF MR systems with comparable diagnostic accuracy for subacute ischemia in humans as that obtained using HF MR despite significantly longer scan time, lower resolution, and generally lower image quality.[33] However lack of resolution is a much more important drawback of LF DWI for small animal patients. In the authors' experience it does not add much to the diagnosis and is currently not recommended for the standard protocol. Similarly, although diffusion tensor imaging, perfusion-weighted imaging, fiber tractography, and functional MR imaging can be performed using LF MR,[1,34–36] routine clinical use of these techniques for humans is restricted to field strengths of 1.5 T and above. The need for higher SNR for these studies is one of the main causes for the trend to higher field strengths in human medicine.[37–40] Molecular imaging and MR spectroscopy also require high field strengths of at least 1 T.[41,42] MR angiography can be performed using LF systems but with relatively poor resolution of intracranial vessels. Conspicuity of intracranial vessels depends greatly on magnetic field strength.[43]

Advantages of LF MR

Cost. Purchase costs for LF MR scanners are considerably lower than for HF systems. LF MR scanners can be installed in smaller rooms, require a smaller Faraday cage, have usually less expensive maintenance contracts, and—in the case of permanent magnets—use less electricity and have no need for liquid helium.[1,2] Furthermore conventional anesthetic and monitoring equipment can be used with LF MR, just placed further from the patient, whereas in a HF environment MR-compatible equipment is mandatory.

Magnet design. Most of the LF magnets have an open design, with easy access to the patient. This facilitates anesthesia monitoring and the possibility of MR-guided procedures.[1,44,45] Reduced susceptibility artifacts associated with LF MR are an advantage when considering interventions.[46]

Safety. MR safety issues can be related to the static magnetic field, the time varying magnetic field, and the radiofrequency (RF) field.[47] The static magnetic field has negligible direct biological effects; however, severe injuries and even lethal accidents have occurred due to the attractive forces of the strong magnetic field on ferromagnetic objects, such as gas bottles or instruments. This force is stronger and potentially more dangerous with HF systems.[48–50]

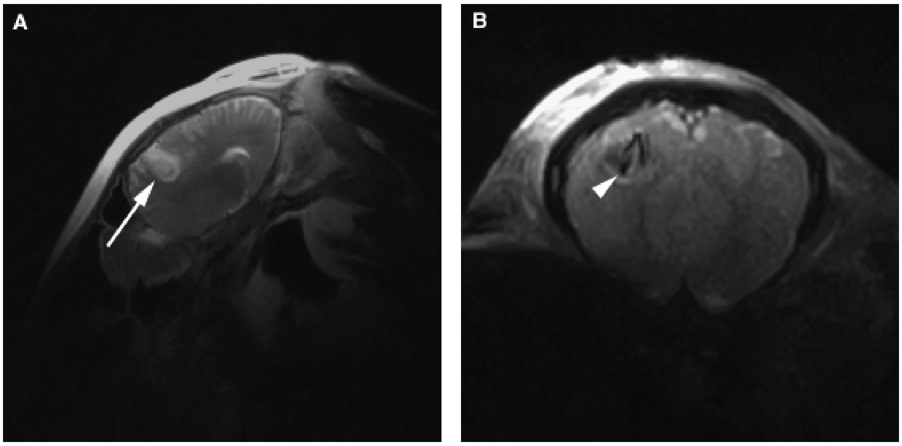

FIG. 1. Swiss Warmblood mare, 185 kg, 4 months: fresh head trauma. (A) Sagittal fast spin echo T2 (TR 4000 ms, TE 100 ms, FA 90°) shows a hyperintense mass lesion in the brain (arrow). (B) T2*-weighted GE image (TR 1037 ms, TE 50 ms, FA 25°) shows a signal void in the center of the lesion caused by a susceptibility artifact associated with the presence of blood degradation products (methemoglobin, hemosiderin). Hematoma was confirmed pathologically. Airis II, 0.3 T.‡ Images courtesy of the MR Center Berne, Vetsuisse Faculty, University of Berne, Switzerland.

Another cause of MR-related injuries is heating of wires (e.g., ECG or pulse oxymetry leads) by RF field-induced currents which has resulted in third degree burns in humans after HF MR imaging.[47,49,51–53] Severe burns have also been caused by direct contact with RF coils or even currents induced by skin contact between limbs.[54,55] No reports of similar incidents could be found for LF MR.

Acoustic noise, which occurs with alterations in the gradient output, is reduced at lower field strengths.[56]

Specific absorption rate (SAR). The FDA limits the maximum level of SAR value to 4 W/kg over 15 min (whole body average).[50] Within these limits the effect on body temperature is negligible during clinical MR imaging. However, it should be noted that there is an exponential relationship between SAR-deposition and field strength: doubling the field strength leads to a fourfold increase in RF power deposition for a given MR pulse sequence.[57] Also, the SAR guidelines were developed for awake adults, and standard MR sequences at higher field strengths can induce clinically significant hyperthermia in sedated children.[58] For veterinary patients that are smaller than children and anesthetized, there is a risk of hyperthermia during HF MR. It is unknown to what extent the effect of SAR-related heating may be counteracted by cooling induced by anesthesia in an air-conditioned environment.

Metallic implants and foreign bodies. Metallic objects inside the body of a patient during MR are subjected to magnetic field interactions (translational attraction and torque), MR-related heating, and induced electrical currents in proportion to the strength of the magnetic field and to the switching rate of the gradients.[42,57] Potentially hazardous heating of a nonferromagnetic stainless steel implant at 1.5 T has been demonstrated during MR imaging using sequences within recommended SAR levels.[59] HF MR should be used with caution in patients known to have metallic implants or suspected of having a foreign body; however, there is the potential for an unexpected metallic inclusion in any patient.[60] The main concern about metallic implants in LF MR is the potential for image artifacts rather than harm to the patient.

Image Artifacts

Although many types of image artifacts affect both LF and HF magnets, certain artifacts are more likely to be encountered during LF MR imaging. For example, motion artifacts occur independently of field strength, but the techniques to overcome them require increased imaging time (gating) or very fast sequences,[61–64] hence reduction of motion artifact is more readily achieved using HF MR.[47,65,66] Truncation (Gibbs) artifacts[47,67,68] are a result of insufficient data sampling which can occur in frequency and phase encoding direction. For in LF MR imaging a smaller number of phase encoding steps is a popular option to save time, this artifact will be seen more often in LF systems.[65] The partial volume artifact can be seen when tissues of different signal intensity become part of the same voxel.[66,68] This artifact also occurs in HF MR[69] but is more of a problem when using thicker image slices, as is often the case in LF MR.

Certain artifacts are reduced when using LF MR. For example, spatial misregistration of fat signal at tissue borders (chemical shift) is directly proportional to the field strength and therefore much more obvious in HF MR imaging.[47,65,66] Also, susceptibility artifacts in the vicinity of air- or bone-tissue interfaces or metallic implants are less marked in LF than HF MR.[30,66,70]

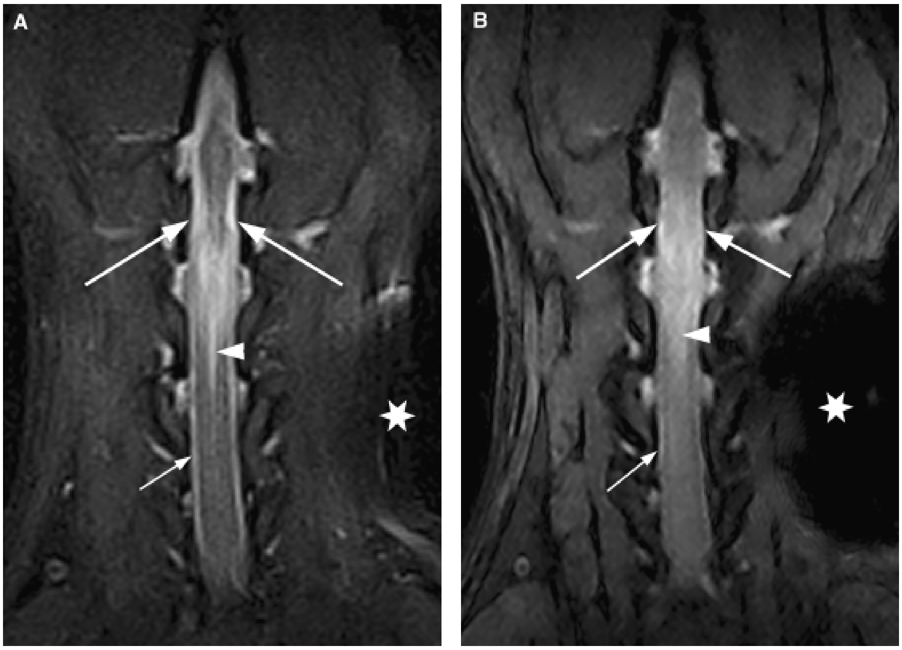

FIG. 2. Mixed breed dog, female, 18 kg, 5 years: Dorsal short tau inversion recovery (STIR) images of a subarachnoid cyst at the level of C3 (large arrows). (A) Fast STIR (TR 3920 ms, TE 30 ms, TI 80 ms); (B) GE STIR (TR 1780 ms, TE 25 ms, TI 75 ms). Both sequences have a slice thickness of 4 mm, but the Fast STIR has higher in plane resolution (matrix 256 × 240) than the GE (matrix 224 × 140). Acquisition time was approximately the same (around 5:30 min) for both sequences. Higher spatial resolution and better fluid/spinal cord contrast allow for a better delineation of the spinal cord (small arrows) and differentiation of the widened central canal (arrow heads) and the intramedullary edema caudally to the cyst. Note the higher sensitivity to the microchip artifact of the GE STIR sequence (asterisk). VetMR Grande 0.25 T.§ Images courtesy of Dr. Zeira, Ospedale Veterinario San Michele, Tavazzano con Villavesco, LO, Italy.

Pulse Sequences in LF MR Neuroimaging

Spin Echo (SE) and Fast Spin Echo (FSE)

As in HF MR, the classical SE is usually only used for T1 weightings. All current LF MR systems offer FSE (aka turbo spin echo) for T2 and/or proton density weighted imaging. FSE enables shorter scan times, which facilitates increased patient throughput or can be translated into images with higher resolution and fluid contrast.[41,42,71–73]

Fat Suppression Techniques[73]

The difference in precessional frequency (3.5 ppm) between fat and water is too small in LF MR imaging to allow selective chemical saturation (spectral fat suppression), hence this method cannot be used in LF MR.[74] Instead fat suppression is accomplished using the short tau inversion recovery (STIR) sequence or the Dixon fat–water separation technique.

STIR is a robust fat-suppressing technique with high sensitivity for fluid and pathology.[73–76] As an inversion recovery sequence the STIR gives low SNR; however, the contrast to noise ratio is excellent.[74] With Fast STIR, signal and contrast can be further improved (Fig. 2).[77–79] Furthermore STIR can be used to achieve excellent gray/white matter contrast (Fig. 3).

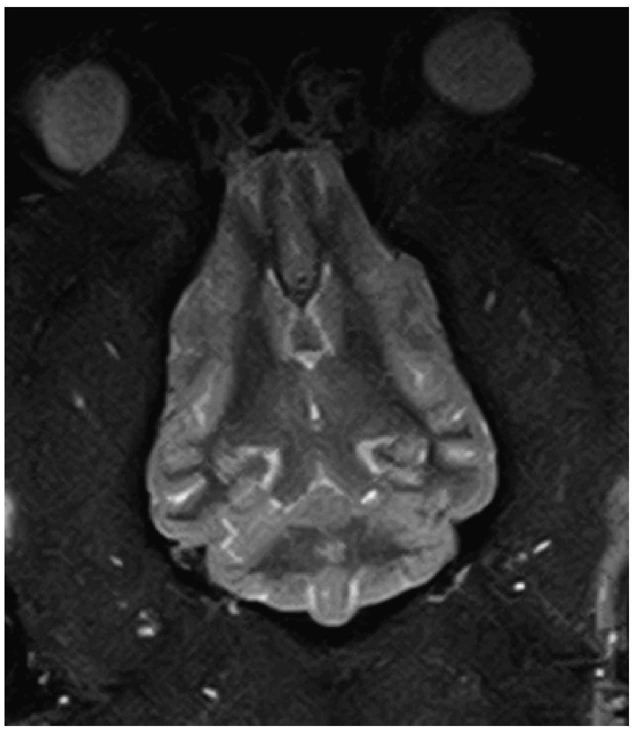

FIG. 3. Entlebucher Sennenhund, female, 25 kg, 8 years. A dorsal Fast short tau inversion recovery (STIR) image (TR 3500 ms, TE 25 ms, TI 110 ms) through the brain at the level of the thalamus provides excellent gray/white matter contrast. Aperto 0.4 T.‡ Image courtesy of Dr. Tassani-Prell, Tierklinik Hofheim, Hofheim, Germany.

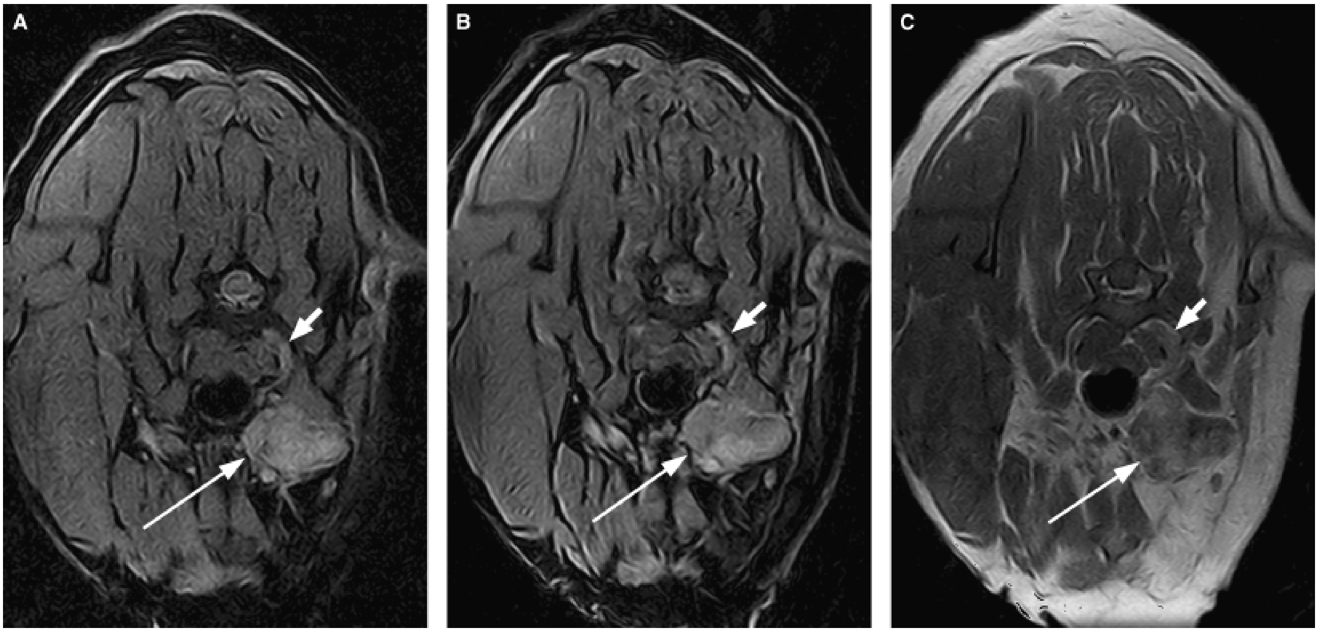

FIG. 4. Mixed breed dog, male, 12 kg, 10 years. Transverse images at the level of C7 showing a suspected peripheral nerve sheath tumor. (A) Dixon fat-saturated T2* (TR 1200 ms, TE 14/28 ms, FA 30°); (B) Dixon fat-saturated T1 + C (TR 600 ms, TE 14/28 ms, FA 90°); (C) Spin echo (SE) T1 + C (TR 450 ms, TE 24 ms; FA 90°). The mass (large arrow) is equally well delineated in the T2* and T1 fat-saturated, less well in the SE T1 postcontrast image. Extension of the lesion proximally along the nerve is better delineated in the fat-suppressed images (small arrow). VetMR Grande 0.25 T.§ Images courtesy of Dr. Zeira, Ospedale Veterinario San Michele, Tavazzano con Villavesco, LO, Italy.

The Dixon method of fat suppression uses the difference in precessional frequency of fat and water bound protons by acquiring 2 (two-point Dixon) or 3 (three-point Dixon) echoes at a different time.[73,80,81]At one point in time, fat and water protons are in phase and their signals sum, whereas at another time they are out of phase and their signals cancel. By addition or subtraction of these echoes a water image (fat suppressed) and a fat image can be generated. In this way, fat-suppressed images can be acquired as T2* weightings, producing images sensitive for pathology with good SNR and resolution. When used with T1 weighting after contrast administration, this technique is highly sensitive for contrast uptake in lesions surrounded by fat, for example in the brachial plexus (Fig. 4). Alternatively, image subtraction of a precontrast T1-weighted series from the postcontrast series can provide a similar result with high conspicuity for contrast uptake.[82]

Fluid Attenuation Inversion Recovery (FLAIR)

FLAIR sequences are usually heavily T2-weighted sequences with selective suppression of the high signal from cerebrospinal fluid (CSF).[83] FLAIR images have shown high sensitivity for various brain lesions in humans[83–87] and veterinary patients.[88–90] Although in one study most abnormalities detected by FLAIR imaging were also evident in T2-weighted images,[91] the presenting and other authors consider FLAIR to be an essential part of a routine brain MR protocol[88] because it can highly increase lesion conspicuity (Fig. 5) and it helps characterize lesions with high signal components in T2-weighted images that must be distinguished from CSF. FLAIR can also be used in spinal cord imaging, although its sensitivity has been questioned.[92]

FLAIR imaging requires a long inversion (1–2 s for 0.2–0.4 T) and long repetition time (at least 5 s) resulting in a long sequence time. To minimize the time necessary for FLAIR imaging, the number of acquisitions and/or phase encoding steps may be reduced, but at the expense of lower SNR. Sufficient signal and resolution can be achieved with a sequence duration between 6 and 8 min.

Balanced Steady State Free Precession Sequences (True FISP type)

True FISP is a gradient echo sequence providing contrast depending on the relation of T1 to T2 (signal amplitude $M = 1/2 \times M_0\sqrt{T2/T1}$).[93,94] T2 is quite independent of field strength whereas T1 relaxation is linearly related to field strength, hence this sequence is used more in LF systems. Use of True FISP in HF MR systems is largely restricted to special applications, such as cardiac, angiographic, abdominal, and fetal imaging.[94,95] True FISP provides a high SNR, high-resolution image with good anatomical depiction and bright signal coming from free fluid, for example in the inner ear[96] or the subarachnoid space (Fig. 6). True FISP cannot be used to replace T2 weightings because of its low sensitivity for fluid within

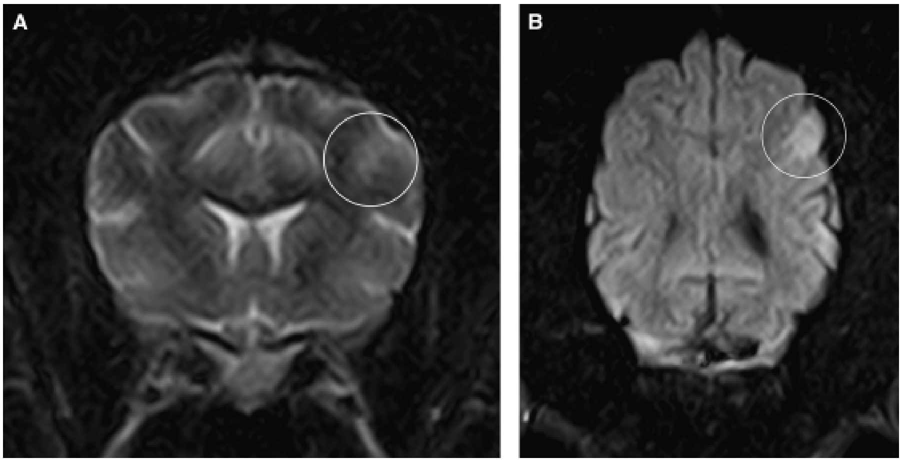

FIG. 5. English Setter, female, 18 kg, 2.5 years. (A) Transverse T2 (TR 7800 ms, TE 120 ms, FA 90°, Echo train 8) through the brain at the level of the caudate nucleus; (B) dorsal fluid attenuation inversion recovery (FLAIR) (TR 5400 ms, TE 100 ms; FA 90°, TI 1350 ms) at the level of the dorsal margins of the lateral ventricles. A hyperintense lesion (circle) is much more conspicuous in the FLAIR image than the T2-weighted image. The same was true for other lesions in this patient. None of the lesions showed contrast uptake (not shown). Diagnosis: granulomatous encephalitis. VetMR Grande 0.25 T.§ Images courtesy of Dr. Zeira, Ospedale Veterinario San Michele, Tavazzano con Villavesco, LO, Italy.

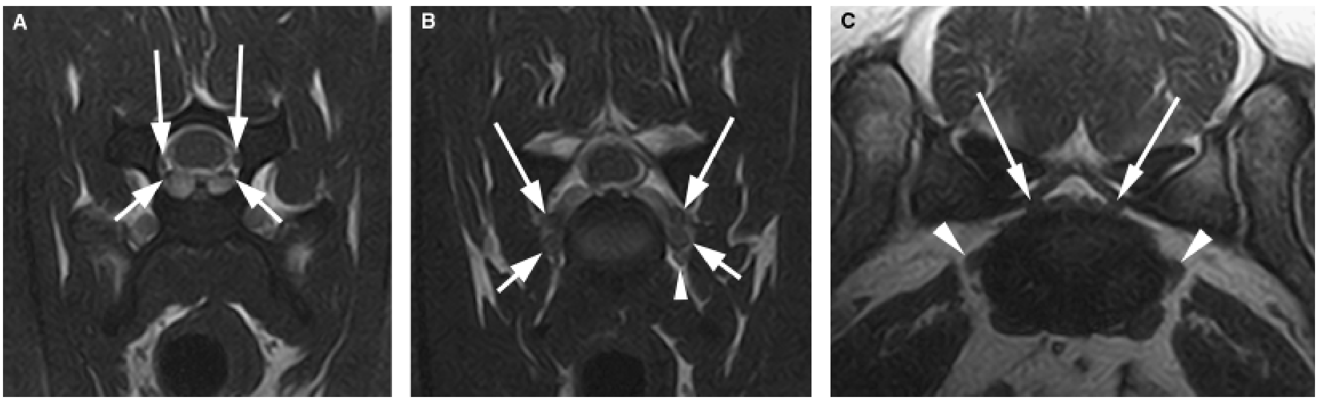

FIG. 6. English Setter, male, 8 years, 30 kg: Normal transverse Hyce three-dimensional (3D) images (TR 10 ms, TE 5 ms, FA 45°; field of view [FOV] 160 × 160, matrix 212 × 199; 1.6 mm slice thickness) at (A) the mid level of C6, depicting the dorsal (long arrows) and ventral (short arrows) roots of the nerves C6 and (B) at the level of the neuroforamina C6/7 where the neural ganglia (long arrows), the vertebral vein (short arrows), and the left sided vertebral artery (arrowhead) are visible. (C) Golden Retriever, male, 45 kg, 9 years, with lumbosacral stenosis: Transverse Hyce 3D (TR 10 ms, TE 5 ms, FA 45°; FOV 160 × 160, matrix 212 × 199; 1.6 mm slice thickness) at the level of L7/S1. The high resolution of this image enables visualization of mild bilateral compression of the S1 nerves (arrows). The L7 nerves can also be seen lateral to the intervertebral disk (short arrows). VetMR Grande 0.25 T.§ Images courtesy of Dr. Zeira, Ospedale Veterinario San Michele, Tavazzano con Villavesco, LO, Italy.

tissues. Another disadvantage is its high sensitivity to field inhomogeneities, which can become problematic when using a large FOV or in the vicinity of metallic objects, e.g. microchips. MR manufactures have invented a confusing range of acronyms for the True FISP sequence (True FISP,* FIESTA,† BASG,‡ Hyce,§ GBASS¶).

*Siemens, Erlangen, Germany.
†GE Healthcare, Hamburg, Germany.
‡Hitachi, Düsseldorf, Germany.
§Esaote, Genova, Italy.
¶Paramed, Genova, Italy.

High-Resolution T1-Weighted Three-Dimensional (3D) Gradient Echo

All LF systems allow high-resolution 3D T1-weighted imaging, but because manufacturers invent their own sequence names, the methodology used is difficult to determine.[97,98] In most instances it seems to be an RF-spoiled gradient echo with 3D Fourier transformation.[75,93,97] In LF MR this sequence enables acquisition of isotropic 1 mm slices of the whole brain in <6 min. Because of the high resolution, small and/or subtle contrast uptake can be detected. For example, facial nerve enhancement which has

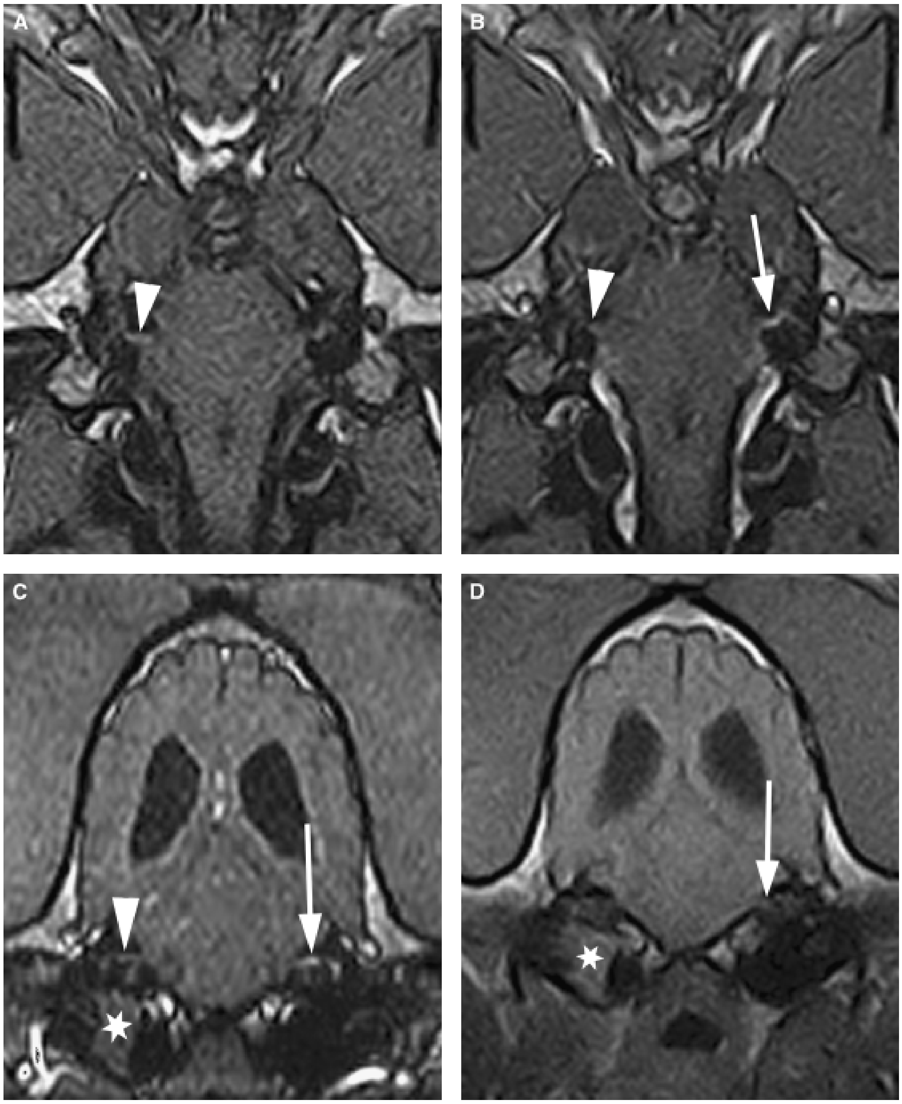

FIG. 7. Boxer dog, male, 30 kg, 7 years with left sided facial nerve paresis. Dorsal Turbo three-dimensional (3D) T1-weighted images of the facial nerve (TR 38 ms, TE 16 ms, FA 65°; field of view [FOV] 190 × 190 mm, matrix 192 × 174; 0.8 mm slice thickness) (A) precontrast; (B) postcontrast; (C) transverse reformat of B. There is enhancement of the left facial nerve (arrow in B and C) but not the right (arrowhead in A–C). (D) Transverse postcontrast spin echo T1-weighted image (TR 600 ms, TE 18 ms, FA 90°; FOV 210 × 210 mm, matrix 256 × 256; 5 mm slice thickness) has insufficient resolution to delineate the enhancing nerve (origin marked with arrow). Material is present in the right tympanic cavity (asterisk in C and D). VetMR 0.2 T.§ Images courtesy of Dr. Harms, Tierklinik Lüneburg; Lüneburg, Germany.

been described at 0.5 T MR imaging on T1-weighted SE[99] can be evaluated with this sequence (Fig. 7).

Contrast Media

Conspicuity of gadolinium-containing contrast media uptake decreases with decreasing field strength,[100–105] hence it has been proposed that the standard human gadolinium dose of 0.1 mmol/kg body weight (BW) should be doubled when using field strengths <0.5 T.[2,106–108] Optimal dose for veterinary patients has not been thoroughly investigated. In the authors' experience, 0.15 mmol/kg BW gadolinium (as diethylenetriaminepentaacetic acid bismethylamide) is satisfactory.

Protocols for Brain and Spine Imaging

Different LF MR systems have specific advantages or disadvantages, and some sequences run better on one system than on another. The following general recommendations are based on many years of experience of LF MR imaging with different machines. The optimal settings for image contrast, slice thickness, and resolution for specific MR systems are not addressed here.

The usual aims in MR imaging are to detect and delineate lesions and to determine their signal intensity in the standard sequences. In general, transverse T2 images are used to delineate lesions with respect to left/right and dorsal/ventral borders, dorsal FLAIR images are used to delineate rostral/caudal borders, and contrast uptake is evaluated with transverse pre- and post-contrast T1-weighted images. This basic protocol leaves enough time for additional sequences to address specific questions related to the anatomical region or suspected pathology.

The authors' standard brain imaging protocol includes FSE T2 in transverse and sagittal plane, dorsal FLAIR, dorsal True FISP, transverse GE T1 or SE T1, and dorsal high-resolution 3D T1 images, both before and after and contrast administration. An average sequence time of 6 min results in total of 48 min for this protocol. With a few additional minutes for sequence planning, a practical total examination time of 60 min is required for the brain.

A minimal spine protocol for a dog with suspected intervertebral disc prolapse includes sagittal T2 and transverse FISP images. In any case a dorsal STIR should be included to exclude bone marrow and muscular pathologies, which could easily be missed in the other two sequences. A more thorough examination of the spine would include transverse T2 images (mainly for intramedullary lesions), transverse SE T1 and dorsal high-resolution 3D T1 images before and after contrast administration. For animals in which imaging of the entire spine is requested, sagittal T2 and dorsal STIR images is an expedient approach that enables most lesions to be excluded, although the small percentage of lesions that are visible only on postcontrast T1 images will be missed.

Summary

Field strength is not everything. Magnetic field homogeneity, gradient strengths and slew rate, coil design, scanner software, and operator skill also influence image quality.[1,2] A modern LF MR imaging can produce images of equal or even better diagnostic quality than an old HF system (e.g., compared with Kraft and colleagues[109,110]). LF MR will continue to dominate veterinary practice, although the trend for increasing field strength in academic institutions may lead to a divergence between what is possible in a research setting and what is needed in practice to improve diagnostic capability for the "average" veterinary patient.

ACKNOWLEDGMENT

Disclosure: The authors declare no conflict of interest.

REFERENCES

1. Hayashi N, Watanabe Y, Masumoto T, et al. Utilization of low-field MR scanners. Magn Reson Med Sci 2004;3:27–38.

2. Marti-Bonmati L, Kormano M. MR equipment acquisition strategies: low-field or high-field scanners. Eur Radiol 1997;7(Suppl 5):263–268.

3. Baeumlin Y, De Rycke L, Van Caelenberg A, Van Bree H, Gielen I. Magnetic resonance imaging of the canine elbow: an anatomic study. Vet Surg 2010;39:566–573.

4. De Decker S, Gielen IM, Duchateau L, Polis I, van Bree HJ, Van Ham LM. Agreement and repeatability of linear vertebral body and canal measurements using computed tomography (CT) and low field magnetic resonance imaging (MRI). Vet Surg 2010;39:28–34.

5. De Decker S, Gielen IM, Duchateau L, et al. Low-field magnetic resonance imaging findings of the caudal portion of the cervical region in clinically normal Doberman Pinschers and Foxhounds. Am J Vet Res 2010;71:428–434.

6. Forterre F, Gorgas D, Dickomeit M, Jaggy A, Lang J, Spreng D. Incidence of spinal compressive lesions in chondrodystrophic dogs with abnormal recovery after hemilaminectomy for treatment of thoracolumbar disc disease: a prospective magnetic resonance imaging study. Vet Surg 2010;39:165–172.

7. Garosi L, Dawson A, Couturier J, et al. Necrotizing cerebellitis and cerebellar atrophy caused by neospora caninum infection: magnetic resonance imaging and clinicopathologic findings in seven dogs. J Vet Intern Med 2010;24:571–578.

8. Kummeling A, Vrakking DJ, Rothuizen J, Gerritsen KM, van Sluijs FJ. Hepatic volume measurements in dogs with extrahepatic congenital portosystemic shunts before and after surgical attenuation. J Vet Intern Med 2010;24:114–119.

9. Olive J. Distal interphalangeal articular cartilage assessment using low-field magnetic resonance imaging. Vet Radiol Ultrasound 2010;51:259–266.

10. Powell SE, Ramzan PH, Head MJ, Shepherd MC, Baldwin GI, Steven WN. Standing magnetic resonance imaging detection of bone marrow oedema-type signal pattern associated with subcarpal pain in 8 racehorses: a prospective study. Equine Vet J 2010;42:10–17.

11. Ricci E, Abbiati G, Cantile C. Intracranial cholesterol granuloma in a cat. J Vet Med Sci 2010;72:1475–1478.

12. Rodriguez MJ, Agut A, Soler M, et al. Magnetic resonance imaging of the equine temporomandibular joint anatomy. Equine Vet J 2010;42:200–207.

13. Zani DD, De Zani D, Morandi N, et al. Imaging diagnosis—split cord malformation. Vet Radiol Ultrasound 2010;51:57–60.

14. Dubrulle F, Delomez J, Kiaei A, et al. Mass screening for retrocochlear disorders: low-field-strength (0.2-T) versus high-field-strength (1.5-T) MR imaging. Am J Neuroradiol 2002;23:918–923.

15. Parizel PM, Dijkstra HA, Geenen GP, et al. Low-field versus high-field MR imaging of the knee: a comparison of signal behaviour and diagnostic performance. Eur J Radiol 1995;19:132–138.

16. Orrison WW Jr, Stimac GK, Stevens EA, et al. Comparison of CT, low-field-strength MR imaging, and high-field-strength MR imaging. Work in progress. Radiology 1991;181:121–127.

17. Gehl HB, Lorch H, Amblank OB, Engerhoff B, Weiss HD. Comparative magnetic resonance imaging of renal space-occupying lesions with a high and low field MRI system. Rofo 1998;169:484–489.

18. Ertl-Wagner BB, Reith W, Sartor K. Low field-low cost: can low-field magnetic resonance systems replace high-field magnetic resonance systems in the diagnostic assessment of multiple sclerosis patients? Eur Radiol 2001;11:1490–1494.

19. Schima W, Wimberger D, Schneider B, Stiglbauer R, Asenbaum S, Imhof H. The importance of magnetic field strength in the MR diagnosis of multiple sclerosis: a comparison of 0.5 and 1.5 T. Rofo 1993;158:368–371.

20. Magee T, Shapiro M, Williams D. Comparison of high-field-strength versus low-field-strength MRI of the shoulder. Am J Roentgenol 2003;181:1211–1215.

21. Rand T, Imhof H, Turetschek K, et al. Comparison of low field (0.2 T) and high field (1.5 T) MR imaging in the differentiation of torned from intact menisci. Eur J Radiol 1999;30:22–27.

22. Murray RC, Mair TS, Sherlock CE, Blunden AS. Comparison of high-field and low-field magnetic resonance images of cadaver limbs of horses. Vet Rec 2009;165:281–288.

23. Nagy A, Dyson S. Magnetic resonance anatomy of the proximal metacarpal region of the horse described from images acquired from low- and high-field magnets. Vet Radiol Ultrasound 2009;50:595–605.

24. Merl T, Scholz M, Gerhardt P, et al. Results of a prospective multicenter study for evaluation of the diagnostic quality of an open whole-body low-field MRI unit. A comparison with high-field MRI measured by the applicable gold standard. Eur J Radiol 1999;30:43–53.

25. Kraft S, Randall E, Wilhelm M, Lana S. Development of a whole body magnetic resonance imaging protocol in normal dogs and canine cancer patients. Vet Radiol Ultrasound 2007;48:212–220.

26. Ripoll MA, Siosteen B, Hartman M, Raininko R. MR detectability and appearance of small experimental intracranial hematomas at 1.5 T and 0.5 T. A 6–7-month follow-up study. Acta Radiol 2003;44:199–205.

27. Seidenwurm D, Meng TK, Kowalski H, Weinreb JC, Kricheff II. Intracranial hemorrhagic lesions: evaluation with spin-echo and gradient-refocused MR imaging at 0.5 and 1.5 T. Radiology 1989;172:189–194.

28. Weingarten K, Zimmerman RD, Deo-Narine V, Markisz J, Cahill PT, Deck MD. MR imaging of acute intracranial hemorrhage: findings on sequential spin-echo and gradient-echo images in a dog model. Am J Neuroradiol 1991;12:457–467.

29. Chavhan GB, Babyn PS, Thomas B, Shroff MM, Haacke EM. Principles, techniques, and applications of T2*-based MR imaging and its special applications. Radiographics 2009;29:1433–1449.

30. Farahani K, Sinha U, Sinha S, Chiu LC, Lufkin RB. Effect of field strength on susceptibility artifacts in magnetic resonance imaging. Comput Med Imaging Graph 1990;14:409–413.

31. Nitz WR, Reimer P. Contrast mechanisms in MR imaging. Eur Radiol 1999;9:1032–1046.

32. Parizel PM, Van Riet B, van Hasselt BA, et al. Influence of magnetic field strength on T2* decay and phase effects in gradient echo MRI of vertebral bone marrow. J Comput Assist Tomogr 1995;19:465–471.

33. Mehdizade A, Somon T, Wetzel S, et al. Diffusion weighted MR imaging on a low-field open magnet. Comparison with findings at 1.5 T in 18 patients with cerebral ischemia. J Neuroradiol 2003;30:25–30.

34. Azmi H, Biswal B, Salas S, Schulder M. Functional imaging in a low-field, mobile intraoperative magnetic resonance scanner: expanded paradigms. Neurosurgery 2007;60:143–148.

35. Meindl T, Born C, Britsch S, Reiser M, Schoenberg S. Functional BOLD MRI: comparison of different field strengths in a motor task. Eur Radiol 2008;18:1102–1113.

36. Okada T, Yamada H, Ito H, Yonekura Y, Sadato N. Magnetic field strength increase yields significantly greater contrast-to-noise ratio increase: measured using BOLD contrast in the primary visual area. Acad Radiol 2005;12:142–147.

37. Bammer R, Skare S, Newbould R, et al. Foundations of advanced magnetic resonance imaging. NeuroRx 2005;2:167–196.

38. Mukherjee P, Berman JI, Chung SW, Hess CP, Henry RG. Diffusion tensor MR imaging and fiber tractography: theoretic underpinnings. Am J Neuroradiol 2008;29:632–641.

39. Mukherjee P, Chung SW, Berman JI, Hess CP, Henry RG. Diffusion tensor MR imaging and fiber tractography: technical considerations. Am J Neuroradiol 2008;29:843–852.

40. Nimsky C, Ganslandt O, Fahlbusch R. Comparing 0.2 tesla with 1.5 tesla intraoperative magnetic resonance imaging analysis of setup, workflow, and efficiency. Acad Radiol 2005;12:1065–1079.

41. McRobbie D, Moore E, Graves M, Prince M. MRI from picture to proton, 2nd ed. Cambridge, UK: Cambridge University Press, 2007.

42. Westbrook C, Kaut C, Talbot J. MRI in practice, 3rd ed. Oxford: Blackwell Publishing Ltd, 2005.

43. Rodriguez D, Rylander H, Vigen KK, Adams WM. Influence of field strength on intracranial vessel conspicuity in canine magnetic resonance angiography. Vet Radiol Ultrasound 2009;50:477–482.

44. Lewin JS. Interventional MR imaging: concepts, systems, and applications in neuroradiology. Am J Neuroradiol 1999;20:735–748.

45. Nimsky C, Ganslandt O, Tomandl B, Buchfelder M, Fahlbusch R. Low-field magnetic resonance imaging for intraoperative use in neurosurgery: a 5-year experience. Eur Radiol 2002;12:2690–2703.

46. Frahm C, Gehl HB, Melchert UH, Weiss HD. Visualization of magnetic resonance-compatible needles at 1.5 and 0.2 Tesla. Cardiovasc Intervent Radiol 1996;19:335–340.

47. Zhuo J, Gullapalli RP. The AAPM/RSNA physics tutorial for residents: MR artifacts, safety, and quality control. Radiographics 2006;26:275–297.

48. Colletti PM. Size "H" oxygen cylinder: accidental MR projectile at 1.5 Tesla. J Magn Reson Imaging 2004;19:141–143.

49. Kanal E, Shellock FG, Talagala L. Safety considerations in MR imaging. Radiology 1990;176:593–606.

50. Price RR. The AAPM/RSNA physics tutorial for residents. MR imaging safety considerations. Radiographics 1999;19:1641–1651.

51. Bashein G, Syrory G. Burns associated with pulse oximetry during magnetic resonance imaging. Anesthesiology 1991;75:382–383.

52. Kugel H, Bremer C, Puschel M, et al. Hazardous situation in the MR bore: induction in ECG leads causes fire. Eur Radiol 2003;13:690–694.

53. Shellock FG, Slimp GL. Severe burn of the finger caused by using a pulse oximeter during MR imaging. Am J Roentgenol 1989;153:1105.

54. Knopp MV, Essig M, Debus J, Zabel HJ, van Kaick G. Unusual burns of the lower extremities caused by a closed conducting loop in a patient at MR imaging. Radiology 1996;200:572–575.

55. Shellock FG, Crues JV. MR procedures: biologic effects, safety, and patient care. Radiology 2004;232:635–652.

56. Price DL, De Wilde JP, Papadaki AM, Curran JS, Kitney RI. Investigation of acoustic noise on 15 MRI scanners from 0.2 T to 3 T. J Magn Reson Imaging 2001;13:288–293.

57. Shellock FG, Morisoli S, Kanal E. MR procedures and biomedical implants, materials, and devices: 1993 update. Radiology 1993;189:587–599.

58. Machata AM, Willschke H, Kabon B, Prayer D, Marhofer P. Effect of brain magnetic resonance imaging on body core temperature in sedated infants and children. Br J Anaesth 2009;102:385–389.

59. Muranaka H, Horiguchi T, Usui S, Ueda Y, Nakamura O, Ikeda F. Dependence of RF heating on SAR and implant position in a 1.5 T MR system. Magn Reson Med Sci 2007;6:199–209.

60. Parry AT, Tanner A, Chandler K, Lamb CR. What is your diagnosis? Foreign body. J Am Vet Med Assoc 2010;237:359–360.

61. Boxerman JL, Mosher TJ, McVeigh ER, Atalar E, Lima JA, Bluemke DA. Advanced MR imaging techniques for evaluation of the heart and great vessels. Radiographics 1998;18:543–564.

62. Boxt LM. Cardiac MR imaging: a guide for the beginner. Radiographics 1999;19:1009–1025.

63. Ferrucci JT. Advances in abdominal MR imaging. Radiographics 1998;18:1569–1586.

64. Scott AD, Keegan J, Firmin DN. Motion in cardiovascular MR imaging. Radiology 2009;250:331–351.

65. Arena L, Morehouse HT, Safir J. MR imaging artifacts that simulate disease: how to recognize and eliminate them. Radiographics 1995;15:1373–1394.

66. Bellon EM, Haacke EM, Coleman PE, Sacco DC, Steiger DA, Gangarosa RE. MR artifacts: a review. Am J Roentgenol 1986;147:1271–1281.

67. Lufkin RB, Pusey E, Stark DD, Brown R, Leikind B, Hanafee WN. Boundary artifact due to truncation errors in MR imaging. Am J Roentgenol 1986;147:1283–1287.

68. Taber KH, Herrick RC, Weathers SW, Kumar AJ, Schomer DF, Hayman LA. Pitfalls and artifacts encountered in clinical MR imaging of the spine. Radiographics 1998;18:1499–1521.

69. Cooper JJ, Levine JM, Young BD, Hicks DG, Hoffman A, Bratton G. Imaging diagnosis—magnetic resonance imaging pseudolesion associated with the petrous temporal bone. Vet Radiol Ultrasound 2010;51:39–41.

70. Stadler A, Schima W, Ba-Ssalamah A, Kettenbach J, Eisenhuber E. Artifacts in body MR imaging: their appearance and how to eliminate them. Eur Radiol 2007;17:1242–1255.

71. Plewes DB. The AAPM/RSNA physics tutorial for residents. Contrast mechanisms in spin-echo MR imaging. Radiographics 1994;14:1389–1404.

72. Sage JE, Samii VF, Abramson CJ, Green EM, SmithM, Dingus C. Comparison of conventional spin-echo and fast spin-echo magnetic resonance imaging in the canine brain. Vet Radiol Ultrasound 2006;47:249–253.

73. Tien RD. Fat-suppression MR imaging in neuroradiology: techniques and clinical application. Am J Roentgenol 1992;158:369–379.

74. Delfaut EM, Beltran J, Johnson G, Rousseau J, Marchandise X, Cotten A. Fat suppression in MR imaging: techniques and pitfalls. Radiographics 1999;19:373–382.

75. Bitar R, Leung G, Perng R, et al. MR pulse sequences: what every radiologist wants to know but is afraid to ask. Radiographics 2006;26:513–537.

76. Krinsky G, Rofsky NM, Weinreb JC. Nonspecificity of short inversion time inversion recovery (STIR) as a technique of fat suppression: pitfalls in image interpretation. Am J Roentgenol 1996;166:523–526.

77. Mehta RC, Marks MP, Hinks RS, Glover GH, Enzmann DR. MR evaluation of vertebral metastases: T1-weighted, short-inversion-time inversion recovery, fast spin-echo, and inversion-recovery fast spin-echo sequences. Am J Neuroradiol 1995;16:281–288.

78. Smith RC, Constable RT, Reinhold C, McCauley T, Lange RC, McCarthy S. Fast spin echo STIR imaging. J Comput Assist Tomogr 1994;18:209–213.

79. Weinberger E, Shaw DW, White KS, et al. Nontraumatic pediatric musculoskeletal MR imaging: comparison of conventional and fast-spin-echo short inversion time inversion-recovery technique. Radiology 1995;194:721–726.

80. Dixon WT. Simple proton spectroscopic imaging. Radiology 1984;153:189–194.

81. Zhang W, Goldhaber DM, Kramer DM. Separation of water and fat MR images in a single scan at .35 T using "sandwich" echoes. J Magn Reson Imaging 1996;6:909–917.

82. Lee VS, Flyer MA, Weinreb JC, Krinsky GA, Rofsky NM. Image subtraction in gadolinium-enhanced MR imaging. Am J Roentgenol 1996;167:1427–1432.

83. Hajnal JV, De Coene B, Lewis PD, et al. High signal regions in normal white matter shown by heavily T2-weighted CSF nulled IR sequences. J Comput Assist Tomogr 1992;16:506–513.

84. Barkhof F, Scheltens P. Imaging of white matter lesions. Cerebrovasc Dis 2002;13(Suppl 2):21–30.

85. Kates R, Atkinson D, Brant-Zawadzki M. Fluid-attenuated inversion recovery (FLAIR): clinical prospectus of current and future applications. Top Magn Reson Imaging 1996;8:389–396.

86. Maeda M, Yagishita A, Yamamoto T, Sakuma H, Takeda K. Abnormal hyperintensity within the subarachnoid space evaluated by fluid-attenuated inversion-recovery MR imaging: a spectrum of central nervous system diseases. Eur Radiol 2003;13(Suppl 4):L192–L201.

87. Maubon AJ, Pothin A, Ferru JM, Berger VM, Daures JP, Rouanet JP. Unselected brain 0.5-T MR imaging: comparison of lesion detection and characterization with three T2-weighted sequences. Radiology 1998;208:671–678.

88. Cherubini GB, Platt SR, Howson S, Baines E, Brodbelt DC, Dennis R. Comparison of magnetic resonance imaging sequences in dogs with multi-focal intracranial disease. J Small Anim Pract 2008;49:634–640.

89. Falzone C, Rossi F, Calistri M, Tranquillo M, Baroni M. Contrast-enhanced fluid-attenuated inversion recovery vs contrast-enhanced spin echo T1-weighted brain imaging. Vet Radiol Ultrasound 2008;49:333–338.

90. Kent M, Delahunta A, Tidwell AS. MR imaging findings in a dog with intravascular lymphoma in the brain. Vet Radiol Ultrasound 2001;42:504–510.

91. Benigni L, Lamb CR. Comparison of fluid-attenuated inversion recovery and T2-weighted magnetic resonance images in dogs and cats with suspected brain disease. Vet Radiol Ultrasound 2005;46:287–292.

92. Ross JS. Newer sequences for spinal MR imaging: smorgasbord or succotash of acronyms? Am J Neuroradiol 1999;20:361–373.

93. Chavhan GB, Babyn PS, Jankharia BG, Cheng HL, Shroff MM. Steady-state MR imaging sequences: physics, classification, and clinical applications. Radiographics 2008;28:1147–1160.

94. Scheffler K, Lehnhardt S. Principles and applications of balanced SSFP techniques. Eur Radiol 2003;13:2409–2418.

95. Ertl-Wagner B, Lienemann A, Strauss A, et al. magnetic resonance imaging: indications, technique, anatomical considerations and a review of fetal abnormalities. Eur Radiol 2002;12:1931–1940.

96. Kneissl S, Probst A, Konar M. Low-field magnetic resonance imaging of the canine middle and inner ear. Vet Radiol Ultrasound 2004;45: 520–522.

97. Brown MA, Semelka RC. MR imaging abbreviations, definitions, and descriptions: a review. Radiology 1999;213:647–662.

98. Hitachi Medical Systems. MRI acronym pocket guide. Twinsburg, OH: Hitachi Medical Systems, 2009. Available at http://www.hitachimed.com/products/mri/MRIAcronymGuide/index.html (accessed February 2, 2010)..

99. Varejao AS, Munoz A, Lorenzo V. Magnetic resonance imaging of the intratemporal facial nerve in idiopathic facial paralysis in the dog. Vet Radiol Ultrasound 2006;47:328–333.

100. Elster AD. How much contrast is enough? Dependence of enhancement on field strength and MR pulse sequence. Eur Radiol 1997;7(Suppl 5):276–280.

101. Knauth M, Wirtz CR, Aras N, Sartor K. Low-field interventional MRI in neurosurgery: finding the right dose of contrast medium. Neuroradiology 2001;43:254–258.

102. Lindsey RO, Yetkin FZ, Prost R, Haughton VM. Effect of dose and field strength on enhancement with paramagnetic contrast media. Am J Neuroradiol 1994;15:1849–1852.

103. Rinck PA, Muller RN. Field strength and dose dependence of contrast enhancement by gadolinium-based MR contrast agents. Eur Radiol 1999;9:998–1004.

104. Yuh WT, Tali ET, Nguyen HD, Simonson TM, Mayr NA, Fisher DJ. The effect of contrast dose, imaging time, and lesion size in the MR detection of intracerebral metastasis. Am J Neuroradiol 1995;16:373–380.

105. Yuh WT, Parker JR, Carvlin MJ. Indication-related dosing for magnetic resonance contrast media. Eur Radiol 1997;7(Suppl 5):269–275.

106. Brekenfeld C, Foert E, Hundt W, Kenn W, Lodeann KP, Gehl HB. Enhancement of cerebral diseases: how much contrast agent is enough? Comparison of 0.1, 0.2, and 0.3 mmol/kg gadoteridol at 0.2 T with 0.1 mmol/kg gadoteridol at 1.5 T. Invest Radiol 2001;36:266–275.

107. Chang KH, Ra DG, Han MH, Cha SH, Kim HD, Han MC. Contrast enhancement of brain tumors at different MR field strengths: comparison of 0.5 T and 2.0 T. Am J Neuroradiol 1994;15:1413–1419.

108. Desai NK, Runge VM. Contrast use at low field: a review. Top Magn Reson Imaging 2003;14:360–364.

109. Kraft SL, Gavin PR, DeHaan C, Moore M, Wendling LR, Leathers CW. Retrospective review of 50 canine intracranial tumors evaluated by magnetic resonance imaging. J Vet Intern Med 1997;11: 218–225.

110. Thomas W, Wheeler S, Kramer R, Kornegay J. Magnetic resonance imaging features of primary brain tumors in dogs. Vet Radiol Ultrasound 1996;37:20–27.